Energy Advances

ROYAL SOCIETY OF CHEMISTRY

PAPER

View Article Online
View Journal | View Issue

Check for updates

Cite this: *Energy Adv.*, 2023, 2, 1045

D–π–A organic dyes derived from the indacenodithiophene core moiety for efficient dye-sensitized solar cells†

Afzal Siddiqui,[ab] Nanaji Islavath,[a] T. Swetha[a] and Surya Prakash Singh *[ab]

Received 3rd February 2023,
Accepted 24th May 2023

DOI: 10.1039/d3ya00060e

rsc.li/energy-advances

We have designed and synthesized two organic sensitizers that have a D–π–A-type architecture based on an indacenodithiophene core with different donor antennas (triphenylamine and phenothiazine). These were then used as light-harvesting materials in dye-sensitized solar cell (DSSC) applications. The electrical and optical properties of the sensitizers were tuned by changing the donor part in the organic D–π–A system. The solar cells with the triphenylamine antenna showed a higher photocurrent density (J_{sc}) of 23.01 mA cm^{-2}, an open-circuit voltage (V_{oc}) of 0.659 V, and more durability than the phenothiazine-based cells (21.47 mA cm^{-2}, 0.640 V), which was due to their band alignment and higher electrical properties. Organic dyes derived from the indacenodithiophene core with a triphenylamine antenna have drawn great interest in academia.

1. Introduction

Considering the disadvantages of commercial silicon solar cells, such as being opaque, heavy in weight, and requiring a costly manufacturing process, much research effort has been devoted to the development of novel photovoltaic technologies.[1] In this context, significant progress has been achieved for dye-sensitized solar cells (DSSCs),[2,3] bulk heterojunction (BHJ) solar cells,[4] and perovskite solar cells (PSCs).[5,6] Among these, DSSC technology has attracted more attention due to the low manufacturing costs involved, the variety of processing techniques and the environmental safety features, as well as the lightweight, colorful, and transparent properties of the cells. In DSSCs, metal-free organic photosensitizers have been shown to be very promising. The best power conversion efficiency (PCE) values for DSSC devices lie in the range of 10–14%.[7–10] Among the various components of DSSCs, photosensitizers play a major role in the performance of DSSC devices. The best champion sensitizers in terms of their performance are Ru-polypyridyl compounds. Considering the real-world application of DSSCs, Ru-based sensitizers present certain disadvantages, such as a low molar extinction coefficient, scarcity, a difficult purification process, and environmental hazards. To overcome these drawbacks, metal-free organic sensitizers have drawn great attention since they have various advantages over metal-based dyes, such as the flexibility of their molecular architecture, low toxicity, an environmentally friendly nature, high molar extinction coefficients, and ease of synthesis and purification. Currently, thousands of photosensitizers have been used for DSSCs, and have focused mainly on indoline,[11–13] phenothiazine,[14,15] coumarin,[16,17] carbazole,[18,19] triarylamine,[20–22] and porphyrin.[23–29] The best DSSC performance for an organic sensitizer was reported in early 2015, with the highest PCE of 14.34% from a co-sensitization process using the ADEKA-1 and LEG-4 dyes.[7] The successful design architecture of organic dyes for DSSCs is based on the donor–π-conjugated-bridge/spacer–acceptor (D–π–A) structure.[30] In the D–π–A design, a push–pull structure is formed among the electron donor and electron acceptor, which helps the injection of electrons. Indaceno[2,1-*b*:6,5-*b*′]dithiophene (IDT) and its derivatives have been well recognized for their excellent optoelectronic properties, such as their low degree of energetic disorder, high electron density, and good carrier mobilities. The IDT core molecule consists of five aromatic rings fused into a single unit, providing an extended π-conjugation system and good coplanar features. It can absorb light up to 700 nm; moreover, incorporating various electron-deficient moieties enables its absorption profile to be tuned. To make efficient light-harvesting materials for photovoltaic applications, 2,1,3-benzothiadiazole (BT) is a good acceptor molecule. BT shows a high electron affinity and helps to achieve a high V_{oc}.[31–33] Considering aforesaid mentioned features, IDT core moiety has been incorporated into dyes used for DSSCs.[34]

Triphenylamine (TPA) is an exceptional electron donor and is often used in functional π-conjugated small-molecule PV

[a] *Department of Polymers and Functional Materials, CSIR-Indian Institute of Chemical Technology, Hyderabad 500007, Telangana, India. E-mail: spsingh@iict.res.in*
[b] *Academy of Scientific and Innovative Research (AcSIR), Ghaziabad 201002, India*

† Electronic supplementary information (ESI) available. See DOI: https://doi.org/10.1039/d3ya00060e

materials. The $-OCH_3$ groups of triphenylamine help to enhance the electron delocalization and electron donation ability of the sensitizer. TPA inhibits aggregation due to its non-planar features; it also demonstrates very strong hole-transport characteristics.[35] Phenothiazine (PTZ)-based heteroatom moieties that contain electron-rich nitrogen and sulfur atoms have been used as electron donors in organic solar cell applications. The molecular structure is similar to TPA, where a thiazine moiety links two phenyl units. This bridge helps to enhance the planarity of both aromatic rings, and shows a different electronic structure compared with the TPA moiety.[36,37]

Herein, we present the design and synthesis of two metal-free photosensitizers based on the D–π–A structure, namely **PITB** and **TITB**. The **PITB** sensitizer comprises the IDT-based core moiety connected with phenothiazine (PTZ) as the donor unit; for **TITB**, the triphenylamine (TPA) donor is installed on the IDT core. For both sensitizers, benzothiadiazole is used as an auxiliary acceptor moiety. In this work, we have successfully demonstrated the concept of a new class of photosensitizers. The **TITB**-based solar cells showed a higher efficiency than the **PITB**-based cells, due to the band alignment and faster charge carrier transfer of **TITB**. By comparison, the triphenylamine-based D–π–A organic sensitizer is more chemically/thermally stable and has a better band alignment with the electrolyte and metal oxide layer.

2. Experimental section

2.1 Materials

Transparent titania paste was used to prepare the nanocrystalline TiO_2 layer (MS code MS002010, 18NR-T Greatcell Solar Ltd), platinum paste (MS code MS0006210, PT1 Greatcell Solar Ltd) was used to prepare the cathode layer. 2-Propanol and acetonitrile were obtained from TCI Chemicals, and 4-*tert*-butylpyridine (4-*t*BP) was purchased from Sigma-Aldrich; these were used as received. Purification was carried out using the column chromatography technique.

2.2 PITB/TITB synthesis

The synthetic route to the **PITB** and **TITB** dyes is presented in the ESI.† The characterization data for **PITB** and **TITB**, *i.e.*, $^1H/^{13}C$ NMR, MALDI-TOF, and device fabrication details, are also presented in the ESI.†[38]

3. Results and discussion

In DSSCs, the sensitizer has a substantial effect on the properties, and D–π–A-based dyes have demonstrated a state-of-the-art performance in tuning the energy levels and optical properties of the molecular system.[2] The energy levels minimize the recombination and increase the charge injection rate. Owing to these properties, we have designed and synthesized two new organic photosensitizers with two different electron donors (triphenylamine and phenothiazine), which are denoted **TITB** and **PITB**, respectively. The molecular structures of the **TITB** and **PITB** dyes are displayed in Fig. 1. The synthetic schemes for **TITB** and **PITB** are shown in Fig. S1 (ESI†).

The indacenodithiophene core moiety was synthesized using a previously reported procedure.[39] The starting compound 1,4-dibromo-2,5-dimethylbenzene **1**, when oxidized under reaction conditions (a), gives the intermediate 2,5-dibromoterephthalic acid **2**, the esterification of which gives the intermediate diethyl 2,5-dibromoterephthalate **3** in good yield; **3** is then reacted with tributyl(thiophene-2-yl)stannane *via* the Stille coupling protocol to give diethyl-2,5-di(thiophene-2-yl)terephthalate **4**. 1-Bromo-4-butylbenzene **5** is then reacted with **4** *via* a concerted reaction to provide 4,4,9,9-tetrakis(4-butylphenyl)-4,9-dihydro-*s*-indaceno[1,2-*b*:5,6-*b*]dithiophene **6**. Upon stannylation of **6**, the trimethyl-(4,4,9,9-tetrakis(4-butylphenyl)-4,9-dihydro-*s*-indaceno[1,2-*b*:5,6-*b*]-dithiophene-2-yl)stannane **7** is given. Suzuki coupling was performed between 4,7-dibromobenzo[*c*][1,2,5]thiadiazole **8** and (4-(methoxycarbonyl)phenyl)boronic acid **9** to obtain methyl 4-(7-bromobenzo[*c*][1,2,5]thiadiazol-4-yl)benzoate **10**, which reacts further with intermediate **7** *via* Stille coupling to give methyl 4-(7-(4,4,9,9-tetrakis(4-butylphenyl)-4,9-dihydro-*s*-indaceno[1,2-*b*:5,6-*b*]dithiophene-2-yl)benzo[*c*][1,2,5]thiadiazol-4-yl)benzoate **11**. The bromination of **11** was carried out to obtain the mono-brominated intermediate **12** in moderate yield. The incorporation of different electron donors onto intermediate **12** *via* Suzuki-coupling enabled us to obtain intermediates **14** and **17**. The hydrolysis of compounds **14** and **17** provided the desired sensitizers **TITB** and **PITB**, respectively. The molecular structures of the final products were confirmed using NMR/MALDI-TOF (ESI†).

To investigate the photophysical properties of the sensitizers, we recorded the UV-vis absorbance spectra and the photoluminescence spectra of **PITB** and **TITB** in the toluene

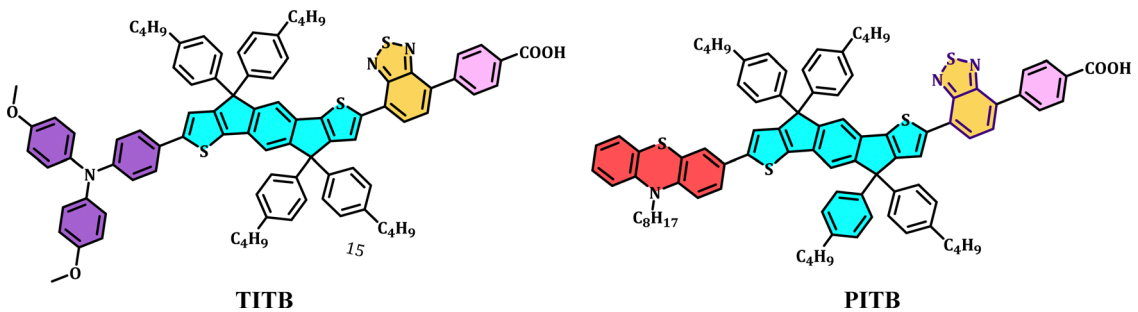

Fig. 1 Molecular structure of the **TITB** and **PITB** dyes.

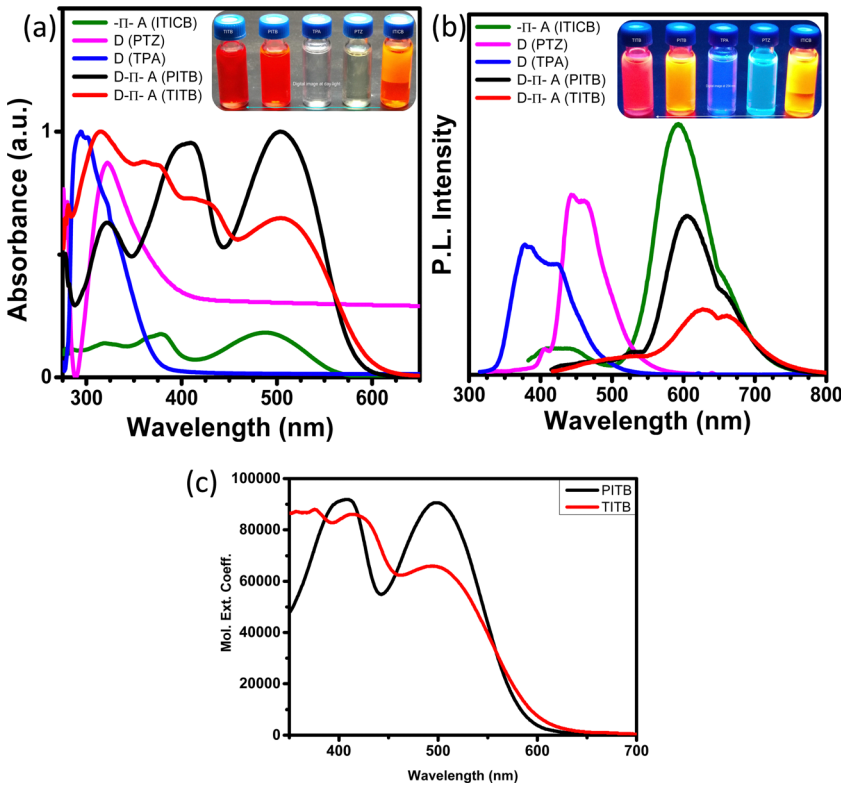

Fig. 2 Normalised (a) absorption and (b) emission spectra of **ITICB**, PTZ, TPA, **PITB**, and **TITB**. (c) Molar extinction coefficient absorption spectra of the **PITB** and **TITB** dyes.

medium. Fig. 2(a) and (b) show, respectively, the absorption and emission spectra of **ITICB** (**12** in the synthetic scheme of the ESI†), *i.e.*, the pre-final product of **PITB** and **TITB**, before and after attachment of the donor moieties. The absorption spectra are shown in the region of 350–570 nm. The donor fragments (triphenylamine and phenothiazine) were attached to the **ITICB** moiety to make the D–π–A organic system to increase the absorption and tune the energy levels associated with traditional electron transporting materials (TiO_2).[40] The sensitizers **PITB** and **TITB** exhibited two notable absorption bands ranging from 280 to 600 nm. However, **TITB** showed a slight redshift in the absorption profile compared with **PITB**. This may be due to the attachment of the TPA moiety. The ICT absorption bands of **TITB** and **PITB** were found at 503 nm and 499 nm, respectively. The low-intensity absorption band can arise from the π–π* transition of the entire D–π–A conjugated backbone. This result indicates the modulation of the optical band gap.[33]

In the toluene solution, the **ITICB** moiety exhibited intense fluorescence under daylight illumination (a red-yellow mixed colour) and a yellow colour under illumination with 254 nm light, probably due to the influence of the acceptor moiety. Both D–π–A organic molecular systems (**PITB** and **TITB**) show very intense fluorescence under daylight as well as 254 nm light illumination (digital photographs are shown in Fig. 3). Subsequently, the emission spectra of these systems before/after the formation of the D–π–A architecture were recorded, and the **ITICB** moiety shows greater emission due to no charge moments from the donor to the acceptor. After attachment of the donor fragments to the **ITICB** moiety, the emission intensity peak reduced by more than 82% for **TITB** and 45% for **PITB** (Fig. 2(c)), and the peak maximum shifted towards the red part of the spectrum; perhaps because of photoinduced electron transfer (PIET) from the donor to the acceptor. The emission spectra reveal that the **TITB** dye exhibits low electron recombination within the molecules, and shows faster charge injection compared with the **PITB** dye. The optical and emission properties of the **PITB** and **TITB** D–π–A dyes reveals that these organic molecular systems are best suited as sensitizers for DSSC applications. It is worth mentioning that, before the attachment of the donor fragments to the **ITICB** moiety, both donor fragments have an absorption only in the region of 290–380 nm, and their emission peak intensity is lower than that of the **ITICB** moiety. The fluorescence properties were varied under daylight (254 nm) and 365 nm illumination.[41] Depending on the light wavelength, a variation in the colour was noticed, and their digital photographs are shown in Fig. S21 (ESI†).

The oxidation (HOMO) and reduction (LUMO) energy levels of the **PITB** and **TITB** sensitizers were recorded using an electrochemical analyzer (three-electrode system).[42] Fig. 4(a) shows the cyclic voltammetry (CV) curves of the **PITB** and **TITB** dyes. Here, ferrocene was used as a reference to calculate the energy level positions (HOMO/LUMO) using the empirical equations of Bredas *et al.*[43] In this case, the triphenylamine-based dye (**TITB**) is easily oxidized and reduced at lower potential values, and its energy levels are well-matched with TiO_2; this is

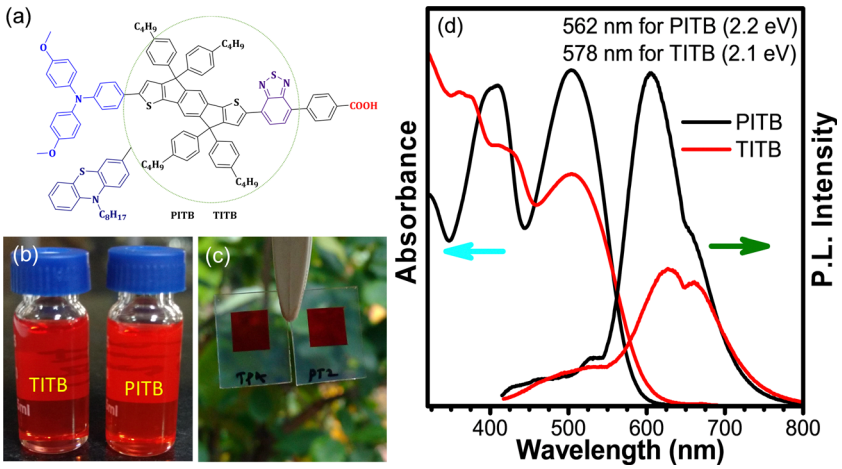

Fig. 3 (a) Molecular structure, (b) and (c) digital photographs of solutions in toluene (b) and films (c), and (d) normalized absorption and PL spectra of the **PITB** and **TITB** dyes in toluene solution.

in contrast with the phenothiazine-based molecular system (**PITB**). The oxidation and reduction energy values of **TITB** (−0.781/+0.692 V) and **PITB** (−0.791/+0.731 V) are shown in Fig. 4(b). We also recorded the thermal stability of the **TITB** and **PITB** sensitizers using thermal gravimetric analysis (TGA) under an argon atmosphere at a heating rate of 10 °C min^{-1}, from 25 to 700 °C. Fig. 4(c) shows the TGA curves of the **PITB** and **TITB** dyes, which show two primary decomposition stages. The first stage, from 40 to 180 °C for **TITB** and from 40 to 160 °C for **PITB**, involves the loss of physically adsorbed moisture. After that, the **PITB** and **TITB** molecules start to decompose (Table 1), and **PITB** shows lower thermal stability compared with **TITB** due to the presence of amines in **PITB**. The amines of **PITB** absorb heat very quickly and start to decompose at low temperatures.

Fig. 5 shows dark current-voltage curves, DSSCs performance of **PITB** and **TITB** measured under 1 Sun irradiation condition (100 mW cm^{-2}, Air Mass 1.5G), and device parameters are listed in Table 1. We recorded the dark-current characteristics of these devices and noticed a specific change in the dark current-voltage curves presented in Fig. 5a. At the

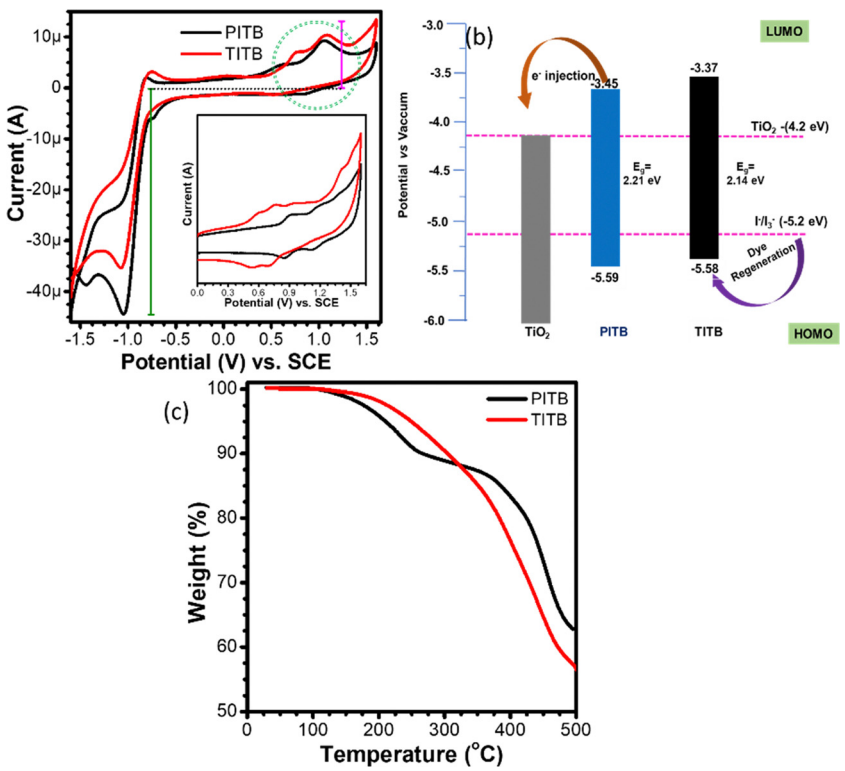

Fig. 4 (a) Cyclic voltammetry and (b) energy level diagram, and (c) thermogravimetric analysis (TGA) of the **PITB** and **TITB** dyes.

Table 1 Optical, TGA and DSSC device performance parameters for **PITB** and **TITB**

Sensitizer	TGA (°C)	λ_{max}[a] (nm)	ε[b] (M^{-1} cm^{-1})	Oxidation potential (V)	Reduction potential (V)	V_{oc} (V)	J_{sc} (mA cm^{-2})	FF	PCE[cd] (%)
PITB	160	499	90 624	−0.781	0.692	0.640	21.47	0.532	7.31
TITB	180	503	65 108	−0.791	0.731	0.659	23.01	0.551	8.35

[a] Absorption wavelength. [b] Molar extinction coefficient values of the sensitizers in toluene solutions at room temperature. [c] Average of 4 cells. [d] Active area = 0.36 cm^2.

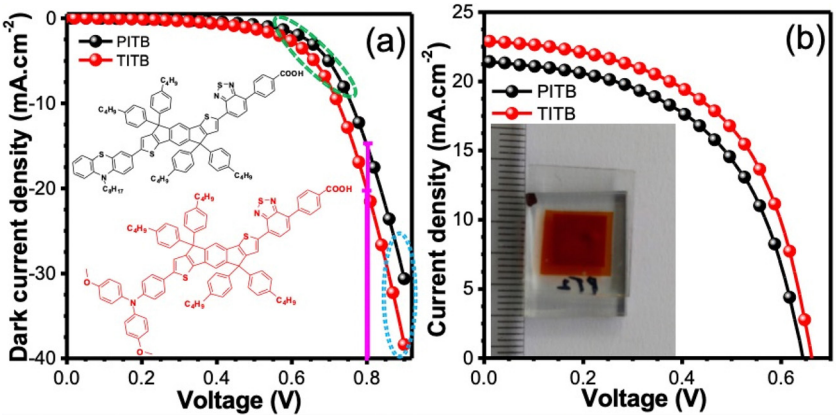

Fig. 5 Characterization of the 0.36 cm^2 active area of the **PITB** and **TIPB** solar cells: (a) dark-current–voltage profile (inset: dye structures), and (b) current–voltage profiles (inset: digital picture of one of the devices).

onset potentials of 0.8 V, the **TITB** device shows higher dark current density compared to the **PITB** devices due to charge separation and injection effect. The dark-current density directly depends on the interface and electrical properties of the light-active materials. The **TITB** devices exhibited a higher short-circuit density (J_{sc}) of 23.01 mA cm^{-2} and open-circuit voltage (V_{oc}) of 0.659 V compared to the **PITB** devices (J_{sc}: 22.47 mA cm^{-2} and V_{oc}: 0.640 V); due to the energy levels and electrical property Fig. 5b. The energy levels and electrical properties of organic sensitizers majorly affect the charge injection and separation in the device. It is worth mentioning that the devices based on **TITB** dye are more stable in iodine (I) based electrolytes as compared to the **PITB**.

4. Conclusion

In summary, we have successfully demonstrated the design and synthesis of two new organic photosensitizers (*i.e.*, metal-free dyes) for DSSCs by incorporating the indacenodithiophene core moiety in the D–π–A structure. In the D–π–A architecture, the indacenodithiophene core moiety was connected with two different donor antennas, triphenylamine and phenothiazine, to produce the respective **TITB** and **PITB** photosensitizer compounds. Their photophysical properties were evaluated and the fabrication of their DSSC devices was carried out. For both dye sensitizers, benzothiadiazole was used as the auxiliary acceptor moiety. Compared with **PITB**, **TITB** is thermally more stable and shows better band alignment with the traditional electron transport material TiO_2, resulting in faster charge injection from the photosensitizer to TiO_2. The **TITB** solar cells showed a higher power conversion efficiency and were more stable in I^-/I_3^- electrolytes. In addition, the **TITB** devices exhibited a higher short-circuit density (J_{sc}) of 23.01 mA cm^{-2}, an open-circuit voltage (V_{oc}) of 0.659 V and an overall power conversion efficiency of 8.35%. By contrast, the **PITB**-based devices showed a J_{sc} of 22.47 mA cm^{-2}, a V_{oc} of 0.640 V, and an efficiency of 7.31%. The device performance of these dyes is many-fold better than several reported metal-based sensitizers. Therefore, we believe that the indacenodithiophene core moiety can be further explored for the preparation of efficient and stable metal-free sensitizers.

Conflicts of interest

There are no conflicts to declare.

Acknowledgements

AS thanks UGC for providing a senior research fellowship. SPS acknowledges financial support from the Government of India, Department of Atomic Energy, BRNS (Sanction no. 58/14/01/2021-BRNS/37065). CSIR-IICT Communication Number: IICT/Pubs./2021/025.

References

1 S. Pizzini, *Sol. Energy Mater. Sol. Cells*, 2010, **94**, 1528–1533.
2 B. O'Regan and M. Grätzel, *Nature*, 1991, **353**, 737–740.

3 M. Kokkonen, P. Talebi, J. Zhou, S. Asgari, S. Ahmed Soomro, F. Elsehrawy, J. Halme, S. Ahmad, A. Hagfeldt and S. Ghufran Hashmi, *J. Mater. Chem. A*, 2021, **9**, 10527–10545.
4 M. Li, W.-H. Chen, M.-T. Lin, I. Oswald, M. Omary and N. D. Shepherd, *J. Phys. D: Appl. Phys.*, 2011, **44**, 365103.
5 M. M. Lee, J. Teuscher, T. Miyasaka, T. N. Murakami and H. J. Snaith, *Science*, 2012, **338**, 643–647.
6 J. Burschka, N. Pellet, S.-J. Moon, R. Humphry-Baker, P. Gao, M. K. Nazeeruddin and M. Grätzel, *Nature*, 2013, **499**, 316–319.
7 K. Kakiage, Y. Aoyama, T. Yano, K. Oya, J. Fujisawa and M. Hanaya, *Chem. Commun.*, 2015, **51**, 15894–15897.
8 S. Mathew, A. Yella, P. Gao, R. Humphry-Baker, B. F. E. Curchod, N. Ashari-Astani, I. Tavernelli, U. Rothlisberger, M. K. Nazeeruddin and M. Grätzel, *Nat. Chem.*, 2014, **6**, 242–247.
9 Z.-F. Yao, J.-Y. Wang and J. Pei, *Chem. Sci.*, 2021, **12**, 1193–1205.
10 Y. Ren, D. Sun, Y. Cao, H. N. Tsao, Y. Yuan, S. M. Zakeeruddin, P. Wang and M. Grätzel, *J. Am. Chem. Soc.*, 2018, **140**, 2405–2408.
11 M. Akhtaruzzaman, A. Islam, F. Yang, N. Asao, E. Kwon, S. P. Singh, L. Han and Y. Yamamoto, *Chem. Commun.*, 2011, **47**, 12400–12402.
12 N. Ohta, K. Awasthi, K. Okoshi, K. Manseki, H. Miura, Y. Inoue, K. Nakamura, H. Kono and E. W. G. Diau, *J. Phys. Chem. C*, 2016, **120**, 26206–26216.
13 J. K. Roy, S. Kar and J. Leszczynski, *J. Phys. Chem. C*, 2019, **123**, 3309–3320.
14 M.-L. Han, Y.-Z. Zhu, S. Liu, Q.-L. Liu, D. Ye, B. Wang and J.-Y. Zheng, *J. Power Sources*, 2018, **387**, 117–125.
15 L. Han, Y. Chen, J. Zhao, Y. Cui and S. Jiang, *Tetrahedron*, 2020, **76**, 131102.
16 S. Martins, J. Avó, J. Lima, J. Nogueira, L. Andrade, A. Mendes, A. Pereira and P. S. Branco, *J. Photochem. Photobiol., A*, 2018, **353**, 564–569.
17 S. Jiang, Y. Chen, Y. Li and L. Han, *J. Photochem. Photobiol., A*, 2019, **384**, 112031.
18 K. S. V. Gupta, J. Zhang, G. Marotta, M. A. Reddy, S. P. Singh, A. Islam, L. Han, F. De Angelis, M. Chandrasekharam and M. Pastore, *Dyes Pigm.*, 2015, **113**, 536–545.
19 P. Naik, M. R. Elmorsy, R. Su, D. D. Babu, A. El-Shafei and A. V. Adhikari, *Sol. Energy*, 2017, **153**, 600–610.
20 K. Narayanaswamy, T. Swetha, G. Kapil, S. S. Pandey, S. Hayase and S. P. Singh, *Electrochim. Acta*, 2015, **169**, 256–263.
21 S. P. Singh, M. S. Roy, K. R. J. Thomas, S. Balaiah, K. Bhanuprakash and G. D. Sharma, *J. Phys. Chem. C*, 2012, **116**, 5941–5950.
22 Y. K. Eom, I. T. Choi, S. H. Kang, J. Lee, J. Kim, M. J. Ju and H. K. Kim, *Adv. Energy Mater.*, 2015, **5**, 1500300.
23 J. V. S. Krishna, D. Koteshwar, T. H. Chowdhury, S. P. Singh, I. Bedja, A. Islam and L. Giribabu, *J. Mater. Chem. C*, 2019, **7**, 13594–13605.
24 G. D. Sharma, D. Daphnomili, K. S. V. Gupta, T. Gayathri, S. P. Singh, P. A. Angaridis, T. N. Kitsopoulos, D. Tasis and A. G. Coutsolelos, *RSC Adv.*, 2013, **3**, 22412.
25 N. V. Krishna, J. V. S. Krishna, S. P. Singh, L. Giribabu, L. Han, I. Bedja, R. K. Gupta and A. Islam, *J. Phys. Chem. C*, 2017, **121**, 6464–6477.
26 S. H. Kang, M. J. Jeong, Y. K. Eom, I. T. Choi, S. M. Kwon, Y. Yoo, J. Kim, J. Kwon, J. H. Park and H. K. Kim, *Adv. Energy Mater.*, 2017, **7**, 1602117.
27 J.-M. Ji, H. Zhou and H. K. Kim, *J. Mater. Chem. A*, 2018, **6**, 14518–14545.
28 H. Zhou, J.-M. Ji, S. H. Kang, M. S. Kim, H. S. Lee, C. H. Kim and H. K. Kim, *J. Mater. Chem. C*, 2019, **7**, 2843–2852.
29 J.-M. Ji, H. Zhou, Y. K. Eom, C. H. Kim and H. K. Kim, *Adv. Energy Mater.*, 2020, **10**, 2000124.
30 L. Alibabaei, J.-H. Kim, M. Wang, N. Pootrakulchote, J. Teuscher, D. D. Censo, R. Humphry-Baker, J.-E. Moser, Y.-J. Yu, K.-Y. Kay, S. M. Zakeeruddin and M. Grätzel, *Energy Environ. Sci.*, 2010, **3**, 1757–1764.
31 S. Wen, Y. Wu, Y. Wang, Y. Li, L. Liu, H. Jiang, Z. Liu and R. Yang, *ChemSusChem*, 2018, **11**, 360–366.
32 Y. Li, M. Gu, Z. Pan, B. Zhang, X. Yang, J. Gu and Y. Chen, *J. Mater. Chem. A*, 2017, **5**, 10798–10814.
33 J.-H. Chen, C.-H. Tsai, S.-A. Wang, Y.-Y. Lin, T.-W. Huang, S.-F. Chiu, C.-C. Wu and K.-T. Wong, *J. Org. Chem.*, 2011, **76**, 8977–8985.
34 Y. Liu, Y. Cao, W. Zhang, M. Stojanovic, M. I. Dar, P. Péchy, Y. Saygili, A. Hagfeldt, S. M. Zakeeruddin and M. Grätzel, *Angew. Chem., Int. Ed.*, 2018, **57**, 14125–14128.
35 A. Mahmood, *Sol. Energy*, 2016, **123**, 127–144.
36 R. K. Konidena, K. R. J. Thomas, D. K. Dubey, S. Sahoo and J.-H. Jou, *Chem. Commun.*, 2017, **53**, 11802–11805.
37 V. A. Chiykowski, B. Lam, C. Du and C. P. Berlinguette, *Chem. Commun.*, 2017, **53**, 2547–2550.
38 S. Zhang, Y. Qin, J. Zhu and J. Hou, *Adv. Mater.*, 2018, **30**, e1800868.
39 K.-T. Wong, T.-C. Chao, L.-C. Chi, Y.-Y. Chu, A. Balaiah, S.-F. Chiu, Y.-H. Liu and Y. Wang, *Org. Lett.*, 2006, **8**, 5033–5036.
40 C.-Y. Chen, M. Wang, J.-Y. Li, N. Pootrakulchote, L. Alibabaei, C.-H. Ngoc-le, J.-D. Decoppet, J.-H. Tsai, C. Grätzel, C.-G. Wu, S. M. Zakeeruddin and M. Grätzel, *ACS Nano*, 2009, **3**, 3103–3109.
41 Q. Yu, Y.-H. Wang, Z. yi, N. Zu, J. Zhang, M. Zhang and Z. Wang, *ACS Nano*, 2010, **4**, 6032–6038.
42 R. E. M. Willems, C. H. L. Weijtens, X. de Vries, R. Coehoorn and R. A. J. Janssen, *Adv. Energy Mater.*, 2019, **9**, 1803677.
43 J. L. Bredas, R. Silbey, D. S. Boudreaux and R. R. Chance, *J. Am. Chem. Soc.*, 1983, **105**, 6555–6559.